https://doi.org/10.20965/jrm.2014.p0540

Review:

Development of Robotic Unicycles

Hisanobu Suzuki*, Shunji Moromugi, and Takeshi Okura*****

*Olympus Imaging Corp.
2951 Ishikawa-machi, Hachioji, Tokyo 192-8507, Japan
E-mail: hisanobu_suzuki@ot.olympus.co.jp
**Department of Electrical, Electronic, and Communication Engineering, Chuo University
1-13-27 Kasuga, Bunkyo-ku, Tokyo 112-8551, Japan
E-mail: moromugi@elect.chuo-u.ac.jp
***Mitsubishi Electric Corporation
1-3-6 Higashikawasaki-cho, Chuo-ku, Kobe, Hyogo 650-0044, Japan
E-mail: takeshi.okura@eurus.dti.ne.jp
[Received August 31, 2014; accepted September 18, 2014]

This paper introduces the first successful development of a robotic unicycle imitating a human rider. The robot consists of a body supported on a single wheel, a closed linkage on each side of the body to drive the wheel, and a rotor on the top. The effects of the closed link, gyro effect, centrifugal force, and reaction torque of the rotor on the robot's stability and direction were investigated in simulations and experiments. Stability and drive principles of the robotic unicycle were proposed. The unicycle accelerated or decelerated because of the location of the compound center of gravity. Direction control was proposed based on the proposed acceleration control rule and a specified yaw angular velocity. Using that rule, drive simulations of tracing a circle and a "number 8" were conducted. The computer simulations demonstrated stable driving of the robotic unicycle. The experimental evaluation, velocity, and direction control of the robot were also studied. The principles of postural stability and driving of the robotic unicycle were clarified.

Keywords: unicycle, emulation of human unicycle riding, motion control, stability and drive principles, robot

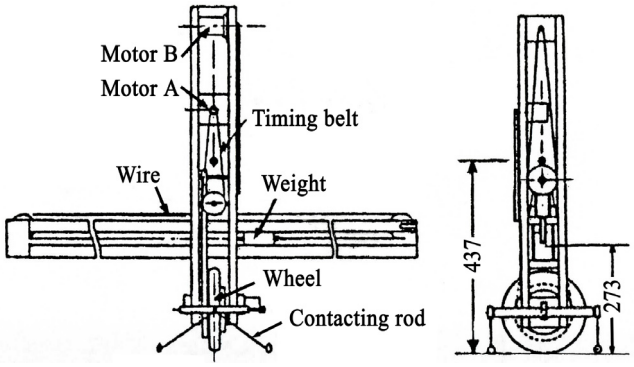

Fig. 1. Unicycle developed by Ozaka et al. [1].

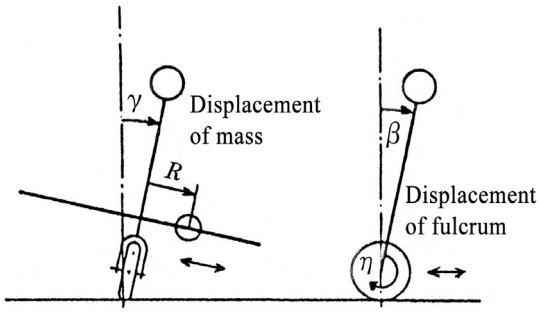

Fig. 2. Modeling by an inverted pendulum and stability principle.

1. Research on Postural Stability and Drive Control of Unicycles

Ozaka et al. [1] developed a unicycle modeled on an inverted pendulum (**Fig. 1**) and analyzed its postural stability and driving, considering pitch (β, longitudinal or forward/backward) and roll (γ, lateral or left/right) motions (**Fig. 2**).

In the experiments, the pitch and roll angles (β and γ) were controlled independently, neglecting mutual interference. Postural stability was achieved by displacing the fulcrum between the inverted pendulum and the ground. Roll was stabilized by moving a weight left or right along the crossbar (**Fig. 2**). Experimental results in posture and unicycle drive control were reported to be successful.

Feng and Yamafuji [2] modeled a unicycle based on an inverted pendulum and conducted computer simulations applying the pole assignment and optimal control to determine the response to external disturbances and stability. Yamafuji and Inoue [3] developed a unicycle controlled by left and right arms that maintained postural stability within 12–13 s, but that turned over when driven forward.

Kawaji et al. [4] tried maintaining postural stability of a unicycle using spin generated by impulsively rotating a balancing arm on top with a horizontal axis.

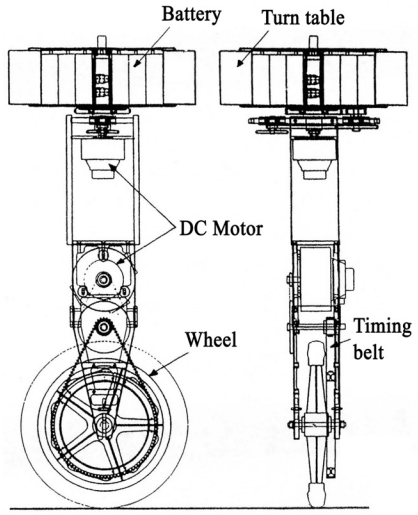

Fig. 3. Unicycle developed by Schoonwinkel [5].

Schoonwinkel [5] developed a unicycle (**Fig. 3**), consisting of a body, a wheel, and a high-speed rotating turntable on top. Batteries were equipped inside the turntable and a controller inside the body. This unicycle depends on the gyro effect of the turntable's rotation and stability owing to the high-speed rotation of the wheel. Thus, it is installed with self-stabilizing equipment. Because we intended to achieve a robotic unicycle without such a self-stabilizing equipment, we considered the similar systems, but free from the gyro-effect, in this study.

2. Robotic Unicycle I: Non-Stand-Alone [6, 7]

The non-stand-alone unicycle was connected to a power source and controller by extended cables, which limited its drive area. The stand-alone model (addressed in Section 3) had a built-in battery and controller. In developing a robotic unicycle, we took videos of a child riding a unicycle and analyzed them. The process and dynamic features are summarized as follows:

1. The unicycle's posture is stabilized by the rider's complex dynamic movement. A unicycle rider maintains longitudinal stability by pedaling faster or slower, by leaning forward or backward, and by extending or contracting the arm.
2. Left and right cranks are rotated alternately. Lateral stability is obtained by steering the wheel in the direction of falling by leaning sideways, extending or contracting the arms, or twisting at the waist.
3. Lateral (right/left) and longitudinal (forward/backward) stability are highly coupled, with lateral stability realized by leaning in a specific direction. Longitudinal control appears to be most important in maintaining postural stability.

Based on these observations, we assumed the following stability and drive processes in unicycle riding:

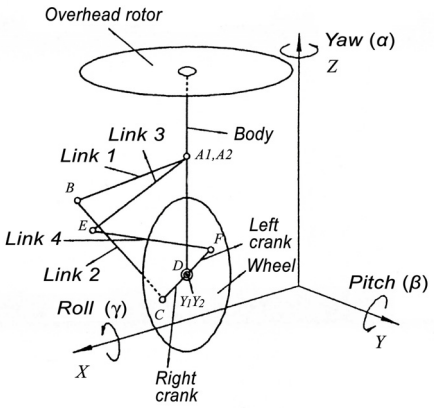

Fig. 4. Model imitating a human riding a unicycle.

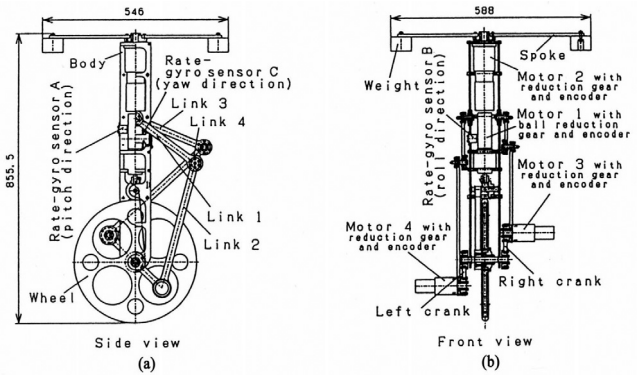

Fig. 5. Developed Unicycle I.

(a) The rider's body, thighs, and shanks and the unicycle cranks form two closed links – a special structure playing a role in controlling unicycle stability, especially longitudinally.

(b) Lateral stability is attained by the rider leaning in the direction of falling.

(c) To change direction or route, the rider leans in the desired direction.

2.1. Robotic Unicycle I

A unicycle model was thus proposed consisting of a wheel, two closed links, and an overhead rotor (**Fig. 4**). **Fig. 5** shows Unicycle I, which consists of a wheel, a body, an overhead rotor, and double closed links. It is driven by four (60 W) motors; motors 1, 3 and 4 drive the unicycle and motor 2 drives the overhead rotor. Three DC servomotors with reduction gears drive the overhead rotor and the two closed links. Motors 2 to 4 have a reduction ratio of 1/50. Motor 1 drives the wheel through a reduction gear with a ratio of 1/45 and a timing belt.

The overhead rotor consists of a hub and three spokes. A 900 g weight is fixed on two tips of the three spokes. The rotor has the same shape as the one-legged mobile robot [8]. Its function is explained in **Fig. 6**, in which **(a)**

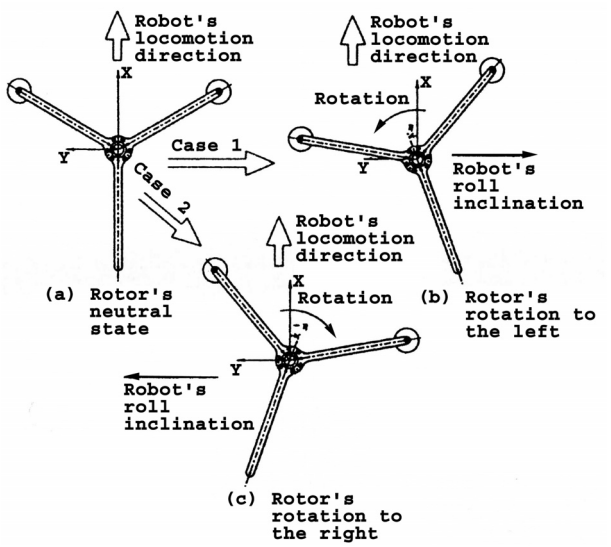

Fig. 6. Overhead rotor's control.

shows the unicycle's stable or initial state without inclination in the roll direction. **Fig. 6(b)** shows how it begins to incline to the right and the rotor rotated counter-clockwise to restore the posture. If it leans to the left, the unicycle restores the posture by rotating the rotor clockwise as shown in **Fig. 6(c)**. This was later verified by simulations and experiments. The unicycle weighs 14.8 kg. Three rate gyro sensors (A, B, and C) measure angular velocity of the body in the pitch (β), roll (γ), and yaw (α) directions. The gyro sensors' resolution is 0.1°/s. An optical encoder (500 pulses/revolution) on each servomotor detects the motor's rotation angle.

We derived the unicycle's postural angles, or Euler angles (α, β, and γ), and angular velocity ($\dot{\alpha}$, $\dot{\beta}$, and $\dot{\gamma}$) using three gyrosensors on the three principal axes of the unicycle for the robot's postural angles (α, β, and γ) and angular velocities (ω_x, ω_y, and ω_z) around the principal axes [9]:

$$\omega_x = \dot{\gamma}\cos\beta - \dot{\alpha}\cos\gamma\sin\beta \quad \ldots\ldots\ldots (1)$$

$$\omega_y = \dot{\beta} + \dot{\alpha}\sin\gamma \quad \ldots\ldots\ldots (2)$$

$$\omega_z = \dot{\gamma}\sin\beta + \dot{\alpha}\cos\gamma\cos\beta. \quad \ldots\ldots\ldots (3)$$

From the angular velocities (ω_x, ω_y, and ω_z) detected by the three gyro sensors, the angular velocities ($\dot{\alpha}$, $\dot{\beta}$, and $\dot{\gamma}$) were obtained using Eqs. (1)–(3), then the Euler angles were derived by integration.

2.2. Unicycle Control Rules

We chose a very simple control rule for the wheel's torque output:

$$\tau_\psi = A \quad \ldots\ldots\ldots\ldots\ldots (4)$$

where τ_ψ is the torque output of motor 1 and A is a constant.

Control rules for crank motors 3 and 4 are the same as proposed elsewhere [6]. Wheel torques provided by the right and left cranks are the same in absolute value, but take an opposite sign because of the opposite motor rotation as shown in **Fig. 4**. Thus:

$$\tau_r = -k_1\beta - k_2\dot{\beta} \quad \ldots\ldots\ldots\ldots (5)$$

and

$$\tau_l = -\tau_r \quad \ldots\ldots\ldots\ldots\ldots (6)$$

where τ_r and τ_l are the torque outputs of motors 3 and 4, and k_1 and k_2 are the feedback gains. As shown in Eq. (5), wheel torque is decided by the pitch angle deviation from zero and its derivative. The most difficult control, i.e., stabilizing the unicycle in the roll direction, is achieved by the overhead rotor. This must be performed quickly to keep the unicycle from falling. From experiments, we found a simple control rule for motor 2 of the overhead rotor:

$$\tau_R = k_3\dot{\gamma} \quad \ldots\ldots\ldots\ldots\ldots (7)$$

where k_3 is the feedback gain.

The unicycle is controlled by applying motor torques based on Eqs. (4)–(7).

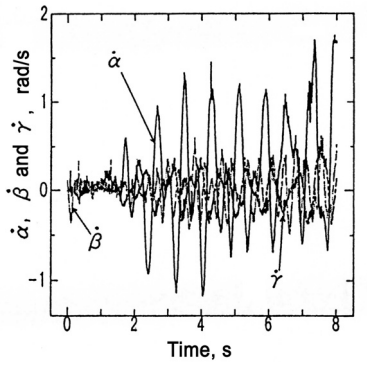

Fig. 7. Experimental results for the unicycle's postural angular velocities, $\dot{\alpha}$, $\dot{\beta}$, and $\dot{\gamma}$.

2.3. Experimental Results for Robotic Unicycle I

Experimental results are presented in **Figs. 7–10**, in which $k_1 = 6{,}000$, $k_2 = 120$, and $k_3 = 2{,}450$ and the sampling interval is 4 ms. **Fig. 7** shows the changes in the unicycle's angular velocity in the yaw ($\dot{\alpha}$), pitch ($\dot{\beta}$), and roll ($\dot{\gamma}$) direction [7]. Changes in postural angles are shown in **Fig. 8**. The posture in the yaw direction changes quickly (**Fig. 8(a)**). Postural stability was realized in the pitch direction (**Fig. 8(b)**). Changes in β remained small, despite large fluctuation. The unicycle drove for 4 s on a 4.5 × 4.5 m rubber carpet laid on the floor. **Fig. 8(c)** shows changes in postural stability in the roll direction.

Figure 9(a) shows changes in the wheel's angular velocity $\dot{\psi}$ and **Fig. 9(b)** the changes in rotational angle ψ. The average robotic unicycle drive speed in the experiment was 1.2 m/s, which is comparable to that of a human rider. **Fig. 10** shows stable Unicycle I driving, with a bumper protecting the wheel.

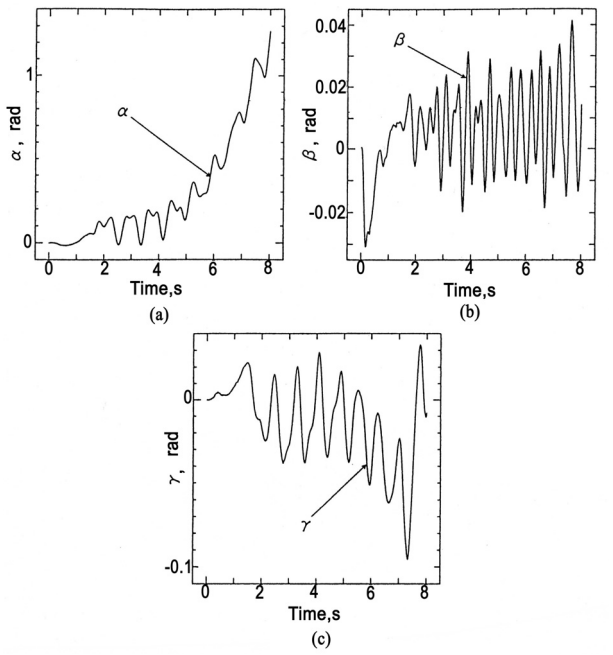

Fig. 8. Experimental results for the unicycle's postural angles, α, β, and γ.

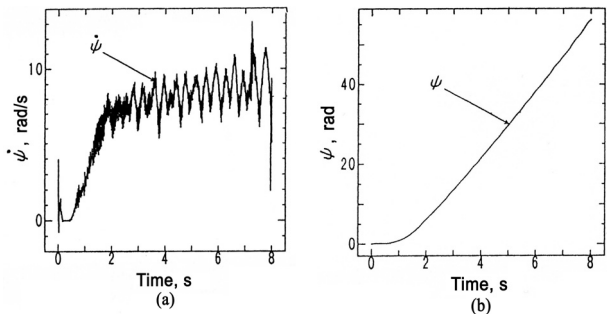

Fig. 9. Changes in wheel angular velocity and rotation angle, $\dot{\psi}$ and ψ.

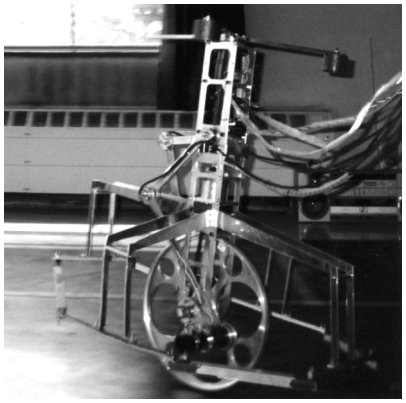

Fig. 10. Robotic Unicycle I in stable driving.

2.4. Unicycle I Simulation Results [7, 10]

Simulations were conducted using the same rules and gains as in the experiments. **Fig. 11** shows the changes in the unicycle's postural angles.

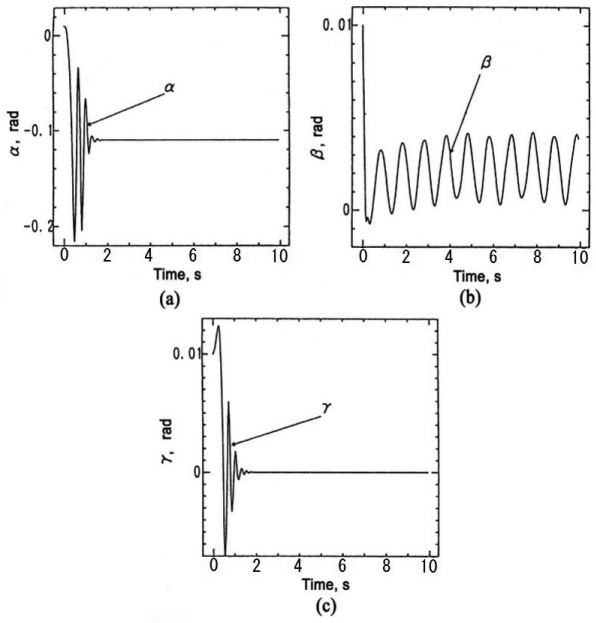

Fig. 11. Simulation results for the unicycle's postural angles, α, β, and γ.

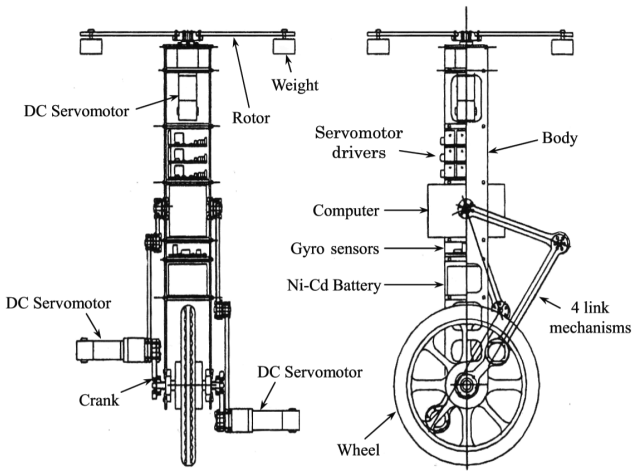

Fig. 12. Developed Unicycle II.

3. Robotic Unicycle II: Stand-Alone [11]

Figure 12 shows the developed robotic Unicycle II. Similar to the non-stand-alone Unicycle I, this prototype uses a closed link on each side of the body and an overhead rotor. Unicycle II has two improvements over Unicycle I: a built-in battery and controller eliminating cables, and a wheel driven by two DC servomotors on double linkages, unlike Unicycle I's one extra motor. Both unicycles use the same overhead rotor driven by a DC servomotor.

All motors have wattage of 60 W with a rotary encoder with a resolution of 500 pulses/revolution. Unicycle II uses three ball reduction gears, two for the cranks (ratio 1/18) and one for the rotor (ratio 1/10). It uses three gyro sensors and an infrared-ray remote controller, which pro-

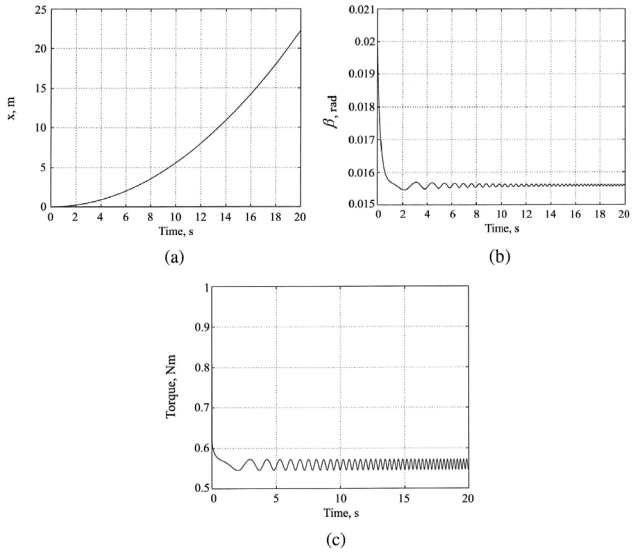

Fig. 13. Simulation results of a 2D model with (a) the wheel rotation distance, (b) the pitch angle, and (c) the wheel torque input.

vides remote control via a microcomputer CARD-486 D4 (CPU, clock 75 MHz). Software is written in Turbo C++ language. Motors are driven by torque commands.

Twelve cadmium-nickel batteries are connected serially. Battery mass is 1.9 kg, nominal-voltage 14.4 V, and electrical capacity 5,000 mAh. The unicycle can be driven for 15 min continuously without battery recharging. Three rate gyro sensors detect the unicycle's three postural angles. An external remote controller (one-chip RISC microcomputer) provides commands for starting and stopping the unicycle.

3.1. A 2D Unicycle Driving Simulation [12]

MATLAB was used to simulate driving a 2D unicycle model with closed linkage. The motor driving the wheel was controlled by a torque command to keep the unicycle upright.

The wheel control torque, τ_w, was calculated based on the following PD control rule:

$$\tau_w = k_{p1}\delta\beta + k_{p2}\delta\dot{\beta} \quad \ldots\ldots\ldots\ldots \quad (8)$$

where k_{p1} is the proportional feedback gain (FBG), k_{p2} the differential FBG, $\delta\beta$ the pitch angle deviation from the target angle, and $\delta\dot{\beta}$ the differential of $\delta\beta$.

Simulation results are shown in **Fig. 13**, with **(a)** the wheel rotation distance, **(b)** the pitch angle, and **(c)** the wheel torque input.

Figure 13 shows successful 2D unicycle driving while maintaining postural stability, even though the pitch angle oscillates in the forward direction. This suggests that stability of the unicycle can be achieved by controlling the wheel.

The drive process of this 2D unicycle can be summarized as follows:

1. The target pitch angle is set slightly larger than zero in the forward direction (**Fig. 14**), so that the unicycle tends to fall forward due to the gravity moment.
2. The wheel is accelerated forward to decrease body tilt.
3. When the unicycle reaches the target pitch angle, the wheel stops accelerating, but the unicycle tends to fall because of the gravity moment.
4. The unicycle is reaccelerated to restore stable posture.
5. The unicycle moves forward by repeating the above sequence.

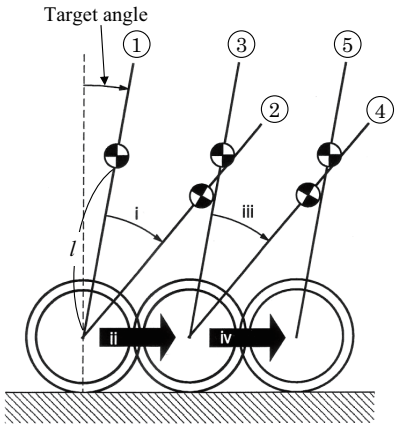

Fig. 14. 2D model in the pitch direction.

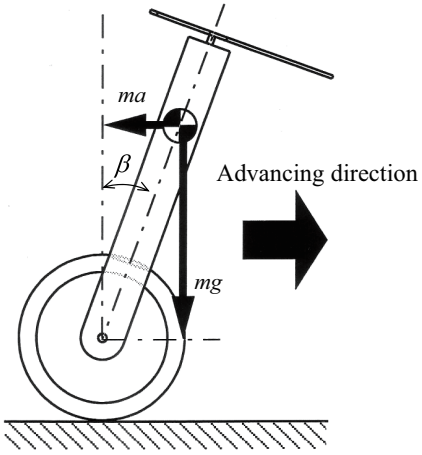

Fig. 15. Force and moment balance in the pitch direction.

The wheel invariably accelerates, and acceleration is calculated from **Fig. 15**. The gravity moment $[mgl\sin\beta]$, letting the machine fall, must be balanced by the inertia moment $[mal\cos\beta]$ from which the wheel's acceleration is derived as $[a = g\tan\beta]$. This means that the more the pitch angle increases, the more acceleration is required.

3.2. Effects of Closed Linkages on Unicycle II [12]

The wheel is driven by two motors on closed linkage cranks. To determine the linkages effects, we developed

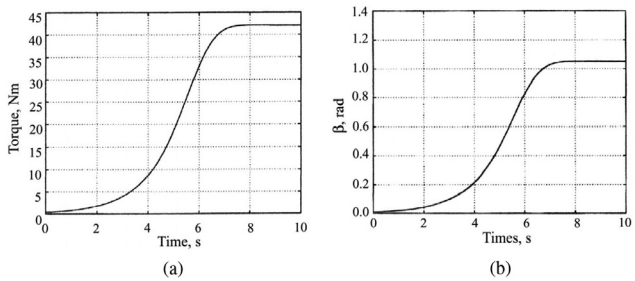

Fig. 16. Changes in torque and pitch angle.

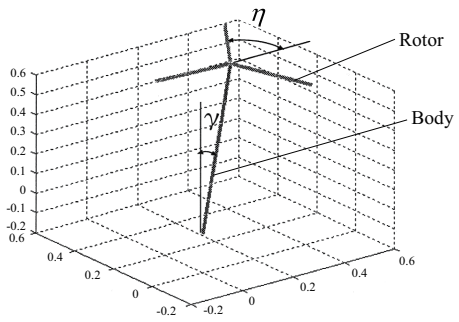

Fig. 17. Inverted pendulum model inclined to the roll direction.

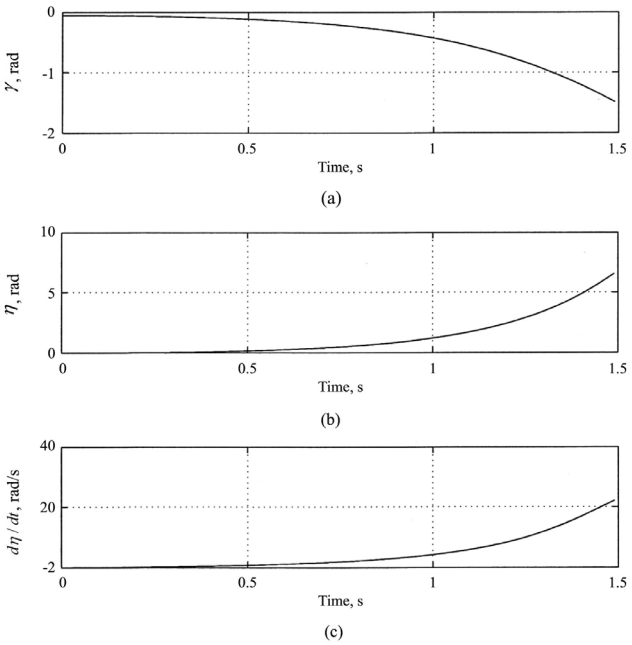

Fig. 18. Effects of rotor rotation on roll angle change with the time history of (a) the roll angle, (b) the rotor rotation angle, and (c) the angular velocity of the rotor.

a computer simulation model in which the wheel is fixed on the ground and the unicycle rotates freely around the wheel axis. In this model, the torque provided by the motors via linkages is fully utilized to rotate the unicycle. Movement was simulated by applying torque to each of the two joints between links 1 and 2, and links 3 and 4.

The same control rule was applied to the linkage motors to maintain a pitch angle of zero. **Fig. 16** shows the changes in the torque and pitch angle. Comparing the torque in **Fig. 13(c)** to that in **Fig. 16(a)**, shows that the torque in **Fig. 13** is too low to keep the unicycle upright. This is because a torque of 4.7 Nm is required to maintain the pitch angle deviation even within 0.1 rad. This means that the unicycle's stability cannot be achieved with the same torque that successfully drove the 2D unicycle previously. Simulation results thus suggest that the linkages effect is low and that most of the motor torque is used for rotating the wheel. We concluded that the effect of the closed linkages on the unicycle is not indispensable.

3.3. Rotor Rotation Stabilization with the Wheel Fixed [12]

To study the rotor rotation effect on unicycle stability in the roll direction, we developed another 2D model to deal with unicycle inclination in the roll direction. This model consisted of an inverted pendulum with its wheel fixed and a rotor on the pendulum, which inclines in the roll direction (**Fig. 17**).

The simulation results in **Fig. 18** show that the pendulum fell despite the rotor rotation. Parametric studies were conducted to test the range of control gain. However, none achieved postural stability in the roll direction, even when the rotor angular velocity was 20 rad/s. Rotor rotation itself therefore does not help to stabilize the unicycle. However, the rotor does play an important role in the stability in the roll direction when the wheel is not fixed as detailed below.

3.4. Wheel and Rotor Rotation Gyro effect [12]

Wheel and rotor rotation may produce a gyro moment in unicycle driving. There exists a relationship given by Eq. (9).

$$M_g = I_r \omega_w \omega_r \quad \ldots\ldots\ldots\ldots\ldots\ldots \quad (9)$$

where ω_w and ω_r are the wheel angular and rotor angular velocity. I_r is the unicycle's moment of inertia at the rotation axis.

When the unicycle leans to the right when moving straight ahead, the wheel and the unicycle turn to the right because of the gyro effect. However, given Eq. (9), the gyro effect is low just after the unicycle starts moving, because the wheel's rotation speed is low. The gyro effect is enhanced as the wheel's angular velocity increases.

3.5. Effect of Varying Forward Direction [12]

Rotor rotation may make the unicycle rotate in the yaw direction, varying the forward direction of the unicycle. Therefore, we studied this effect on unicycle stability through 3D computer simulation. **Fig. 19** shows trajectories of the wheel contact point (CP) with the ground and the compound center of gravity (CCG) [13]. The enlarged graph in **Fig. 19(a)** shows that the unicycle moves forward to the right. The change in the unicycle's forward movement (pitch) and posture inclination (roll) are

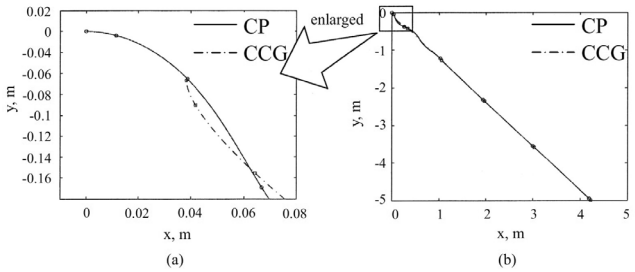

Fig. 19. Trajectories of the CP and CCG, and changes in the forward direction with (a) enlarged trajectories and (b) trajectories.

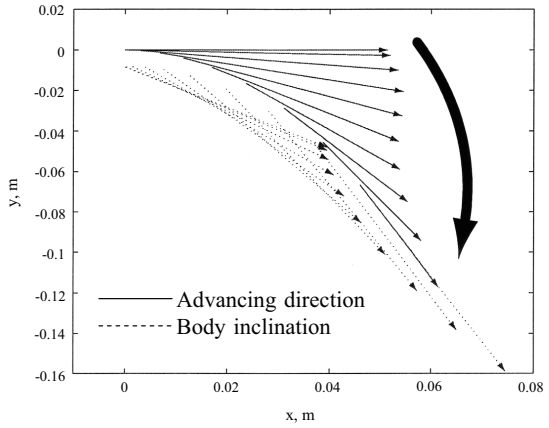

Fig. 20. Vector changes in the forward direction following unicycle inclination.

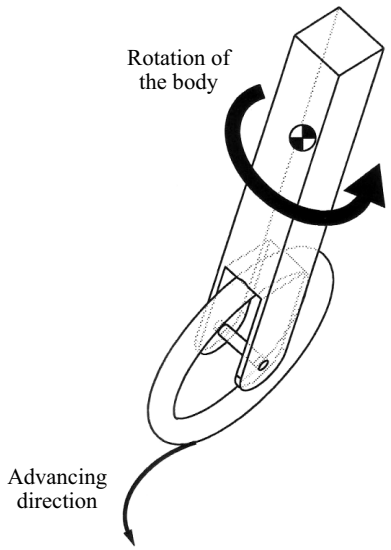

Fig. 21. Stabilization in the roll direction.

expressed by vectors on the ground (**Fig. 20**). The unicycle is kept from falling by changing the forward direction toward tilt (**Fig. 21**). Changes in unicycle inclination toward roll are followed by changing the forward direction, so that stability in the roll direction is attained by cooperative movement caused by the wheel and rotor rotation.

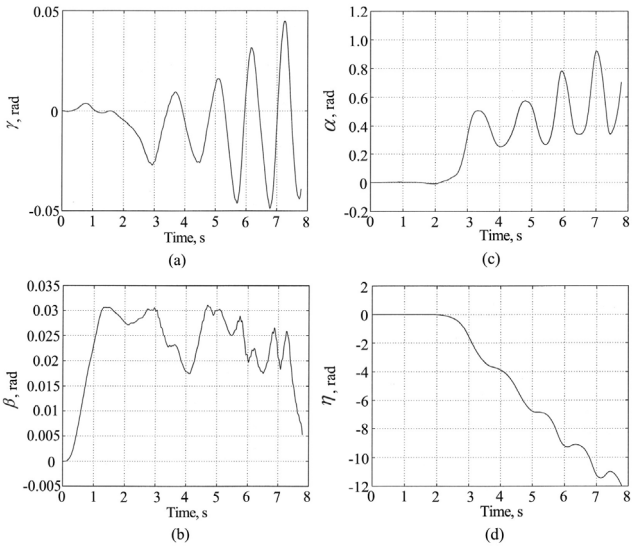

Fig. 22. Experimental results for changes in unicycle angle with (a) the roll, (b) the pitch, (c) the yaw, and (d) the rotor angle.

3.6. Experimental Results [14]

3.6.1. Control Rules

Using fuzzy scheduling controllers developed by Sheng and Yamafuji [15], we conducted experiments on driving Unicycle II. The torque commands for the motors were as follows:

$$\tau_r = -k_1 f_1 \beta - k_2 f_2 \dot{\beta} \quad \ldots\ldots\ldots\ldots \quad (10)$$

$$\tau_l = -\tau_r \quad \ldots\ldots\ldots\ldots\ldots\ldots \quad (11)$$

$$\tau_R = k_3 f_3 \gamma + k_4 f_4 \dot{\gamma} \quad \ldots\ldots\ldots\ldots \quad (12)$$

τ_r and τ_l are the torque commands to the motors on cranks r and l, and τ_R that of the overhead rotor. Gains f_1, f_2, f_3, and f_4 are variables obtained by fuzzy reasoning and changed in real-time based on the instantaneous posture of the unicycle.

3.6.2. Experimental Results

Figure 22 shows the experimental results for changes in roll (γ), pitch (β), yaw (α), and rotor rotation angle (η). Variations in pitch and roll angle are limited to within 0.03 rad and $\pm$0.05 rad. **Fig. 22(b)** shows that Unicycle II driving was stable. Comparing changes in yaw and rotor rotation angle, yaw angle increased in the direction opposite to that of rotor rotation (**Figs. 22(c)** and **(d)**). Note that the inclination in the roll direction was invariably corrected by increasing the yaw angle, i.e., by rotating the unicycle around the yaw angle caused by the reaction of the rotor rotation.

Figure 23 shows the changes in roll and yaw angular velocity. Fluctuation similarities in **Figs. 23(a)** and **(b)** show that they are closely related, because the change in yaw angular velocity is linked to roll velocity. The minor time delay between them implies that the position restoration by the reaction of the rotor rotation takes time. The

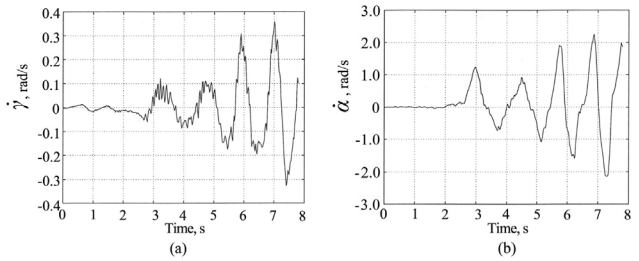

Fig. 23. Changes in (a) roll and (b) yaw angular velocity.

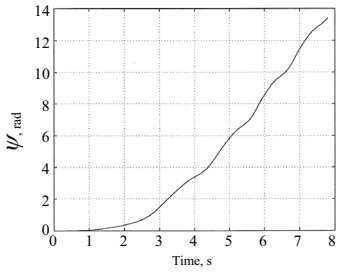

Fig. 24. Changes in wheel angle.

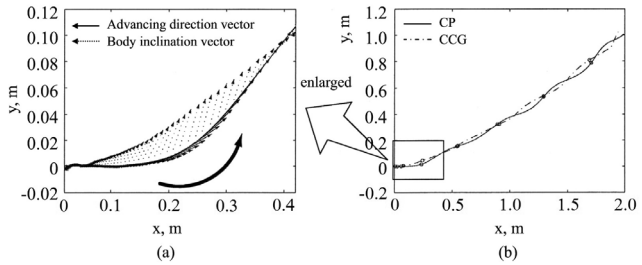

Fig. 25. Changes in (a) direction vector and (b) trajectories of the CP and CCG.

change in the wheel angle in **Fig. 24** shows that wheel rotation was not constant.

3.6.3. Verification of Stability and Driving Principles

Figure 25 shows the CCG trajectories and the unicycle's CP with the ground [13]. **Fig. 25(a)** shows the longer starting period of **Fig. 25(b)**. It is observed that the trajectory changes in such a way that the traveling direction becomes close to the direction of body inclination. Thus, a stable posture is restored. The unicycle restores the posture change by rotating the body. Note the trajectory near a point ($x = 1.5$ m and $y = 0.7$ m) in **Fig. 25(b)** at which the CP and CCG cross and twist together as if making a rope.

The relationship between CP and CCG is shown in **Fig. 26**. **Fig. 26(b)** shows that the trajectories of CP and CCG curve in directions opposite to each other, showing that the unicycle's postural stability is not attained by the centrifugal force. If a centrifugal force acts on the CCG in the trajectory in **Fig. 26(b)**, it does not act in a direction to restore the posture, but in the opposite direction to be detrimental to it. This means that the unicycle's posture is not restored by centrifugal force.

We verified why the CP and CCG curve in a direction

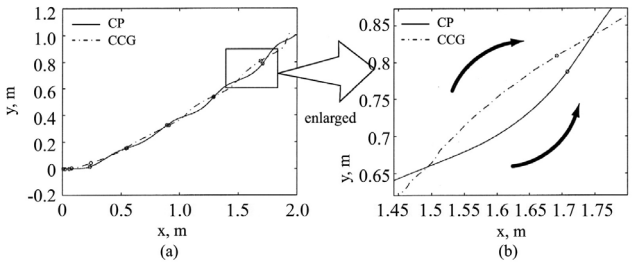

Fig. 26. Relationship between the CP and CCG projected on the ground, with (a) the trajectories of the CP and CCG and (b) an enlargement of (a) near $x = 1.5$ m.

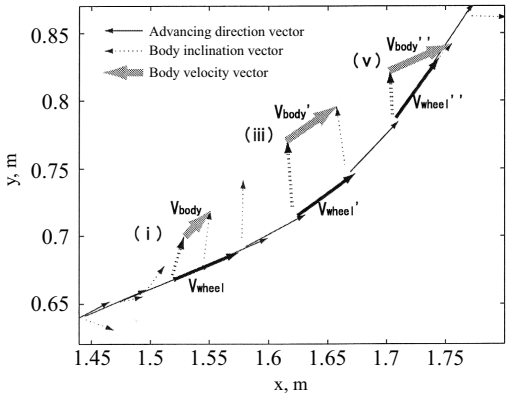

Fig. 27. Vectors of the unicycle's forward and inclination direction projected on the ground.

opposite to each other, while the unicycle's posture could be restored. The wheel's forward direction and the unicycle's inclination in **Fig. 26(b)** are expressed by vectors as shown in **Fig. 27**. It is confirmed that the forward direction vector is followed after the unicycle's inclination as shown by the simulations in Section 3.5. The forward direction vector follows the unicycle's inclination vector.

4. Conclusions on Unicycle Postural Stability and Drive

The following conclusions were drawn from this study [12, 14]:

1. Regarding the unicycle stability principle in the pitch direction, when the unicycle inclines forward more than a fixed angle (target angle in **Fig. 14**), the wheel rotates to catch it and the unicycle is forced to fall due to gravity (**Fig. 15**). The wheel quickly accelerates to restore stability.

2. According to the drive principle, the unicycle accelerates or decelerates based on whether the projection of the CCG on the ground is in front of or behind the CP. Therefore, it can go forward by specifying the pitch angle to let the CCG overlap with the CP. Control based on the location of the CCG and the CP is useful in controlling inverted pendulum vehicles.

3. When the unicycle leans in the roll direction, its inclination is compensated for by the unicycle rotating around the yaw axis by rotating the rotor counterclockwise. The reaction torque of the rotor rotates the unicycle toward inclination.

4. Changes in the unicycle's pitch, roll, and yaw angle are closely interrelated. The unicycle's rotation angle required for restoring the inclination in the roll direction is obtained and corrected using fuzzy scheduling controllers.

5. The role of the overhead rotor is complex and changes the forward direction of the unicycle through its rotation around the yaw axis. It conducts movement dynamically similar to a unicycle rider twisting the torso, extending the arms, and hunching the shoulders.

6. A study of gyro and centrifugal force effects showed that these were negligible compared to those of the reaction torque by rotor rotation and the inertia due to unicycle driving.

7. Closed links were assumed indispensable to unicycle riding. Crank action, however, is not required for the unicycle's postural stability in the pitch direction, so the wheel can be driven directly by a motor without such links.

8. A proposed acceleration control rule [14] requires that a target pitch angle is adjusted based on wheel velocity. Its effectiveness was verified by experiments and computer simulation [14].

9. We proposed a direction control rule combining the acceleration control rule and the specification of the yaw angular velocity. Simulations were conducted satisfactorily with the unicycle tracing a circle and a "number 8." This showed the feasibility of the direction control rule, which can be applied to driving an inverted pendulum robot along a given path at a constant arbitrary velocity. Simulation examples of the direction control are shown in **Figs. 28** and **29** [14].

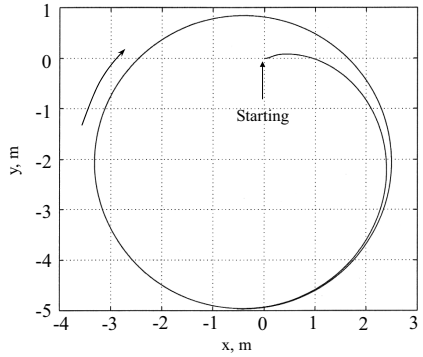

Fig. 28. Trajectories of the traced circle on the ground.

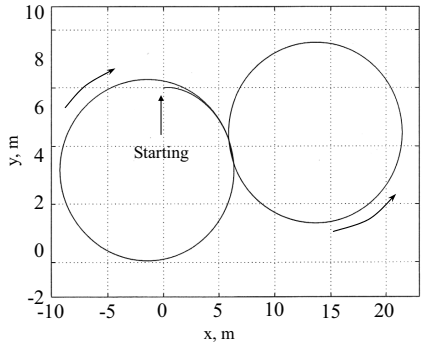

Fig. 29. Trajectories of the traced "number 8" on the ground.

Acknowledgements

The authors thank Professor Yamafuji, Professor Emeritus of the University of Electro-Communications, who supervised this study and also provided advice and materials related to this paper.

References:

[1] C. Ozaka, S. Kano, and M. Masubuchi, "Stability of a monocycle-type inverted pendulum," Proc. of Symposium of Japan Automatic Control Society, pp. 63-66, 1980 (in Japanese).

[2] Q. Feng and K. Yamafuji, "Design and Simulation of a Control System of an Inverted Pendulum," Robotica, Cambridge University Press, Vol.6, No.2, p. 235-241, 1988.

[3] K. Yamafuji and K. Inoue, "Study on the Postural Stability of a Unicycle," Proc. of Annual Yamanashi Meeting of Japan Society of Mechanical Engineers (JSME), pp. 4-6, 1986 (in Japanese).

[4] S. Kawaji, T. Shiotsuki, and N. Matsunaga, "Stabilization of Unicycle Using Spinning Motion," Trans. of Institute of Electrical Engineers of Japan, Vol.107-D, No.1, pp. 21-28, 1987 (in Japanese).

[5] A. Schoonwinkel, "Design and Test of a Computer Stabilized Unicycle," Ph.D. Dissertation, Stanford University, 1987.

[6] Z. Q. Sheng and K. Yamafuji, "Study on the Stability and Motion Control of a Unicycle (Part 1: Dynamics of a Human Riding a Unicycle and its Modeling by Link Mechanisms," JSME Int. J., Series 3, Vol.38, No.2, pp. 249-259, 1995.

[7] Z. Q. Sheng and K. Yamafuji, "Postural Stability of a Human Riding a Unicycle and Its Emulation," IEEE Trans. on Robotics and Automation, Vol.13, No.5, pp. 709-720, 1997.

[8] K. Yamafuji, Y. Takemura, and H. Fujimoto, "Dynamic walking control of the one-legged robot which has the controlling rotor," Trans. of Japan Society of Mechanical Engineers, Vol.57-538C, pp. 1930-1935, 1991 (in Japanese).

[9] S. Koide, "Analytical Dynamics," Iwanami Publ. Ltd., 1983 (in Japanese).

[10] Z. Q. Sheng and K. Yamafuji, "Study on the Stability and Motion Control of a Unicycle (Part 3: Characteristics of a unicycle robot)," JSME Int. J., Series 3, Vol.39, No.3, pp. 560-568, 1996.

[11] K. Ohkura, K. Yamafuji, and T. Tanaka, "Development and Motion Control of a Unicycle Robot without Extension Cables," Proc. of Annual Meeting of Japan Society of Mechanical Engineers (JSME), pp. 1AI3.7(1)-1AI3.7(2), 1998 (in Japanese).

[12] H. Suzuki, S. Moromugi, and K. Yamafuji, "Motion Principle and Control of a Human Riding Type Robotic Unicycle (Part 1, Mechanisms, Stability Principles and Simulation)," Int. J. of Mechanics and Control, Vol.12, No.2, pp. 1-12, 2011.

[13] T. Hirabayashi and K. Yamafuji, "Posture and Driving Control of a Variable Structure Type Parallel Bicycle (1st Report, Upright posture and driving control of an arm-wheel model)," Trans. of JSME, Vol.56, No.523C, pp. 721-730, 1990 (in Japanese).

[14] H. Suzuki, S. Moromugi, and K. Yamafuji, "Motion Principle and Control of a Human Riding Type Robotic Unicycle (Part 2, Motion Principles, Direction Control, Experiments and Simulation)," Int. J. of Mechanics and Control, Vol.12, No.2, pp. 13-20, 2011.

[15] Z. Q. Sheng, K. Yamafuji, and S. V. Ulyanov, "Study on the Stability and Motion Control of a Unicycle (4th report: Fuzzy Gain Schedule PD Controller for Managing Nonlinearity of Systems)," JSME Int. J., Series 3, Vol.39, No.3, pp. 569-576, 1996.

The basis of this paper is Chapter 3 of K. Yamafuji, "Useful Robots and Hopeful Robots," Fuji Technology Press Ltd., 2010.

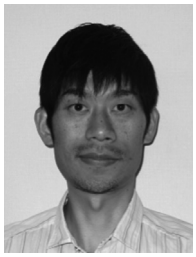

Name:
Hisanobu Suzuki

Affiliation:
Olympus Imaging Corp.

Address:
2951 Ishikawa-machi, Hachioji, Tokyo 192-8507, Japan

Brief Biographical History:
2001- Honda R&D Co., Ltd.
2008- Olympus Imaging Corp.

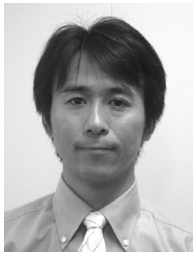

Name:
Shunji Moromugi

Affiliation:
Associate Professor, Department of Electrical, Electronic, and Communication Engineering, Chuo University

Address:
1-13-27 Kasuga, Bunkyo-ku, Tokyo 112-8551, Japan

Brief Biographical History:
2002-2007 Research Associate, Department of Mechanical Systems Engineering, Nagasaki University
2010 Visiting Researcher, Department of Mechanical & Aerospace Engineering, University of California, Irvine, USA
2011 Visiting Researcher, Center for Sensory-Motor Interaction, Aalborg University, Denmark
2007- Assistant Professor, School of Engineering, Nagasaki University
2014- Associate Professor, Department of Electrical, Electronic, and Communication Engineering, Chuo University

Main Works:
• studies on biomedical sensing, wearable robots to extend human ability, surgery robot

Membership in Academic Societies:
• The Institute of Electrical and Electronics Engineers (IEEE)
• The Society of Instrument and Control Engineers (SICE)
• The Japan Society of Mechanical Engineers (JSME)
• The Robotics Society of Japan (RSJ)
• Japanese Society for Medical and Biological Engineering

Name:
Takeshi Okura

Affiliation:
Mitsubishi Electric Corporation

Address:
1-3-6 Higashikawasaki-cho, Chuo-ku, Kobe, Hyogo 650-0044, Japan

Brief Biographical History:
1998- Mitsubishi Electric Corporation